Supporting Information

Beyond slow two-state protein conformational exchange using CEST: Applications to three-state protein interconversion on the millisecond timescale

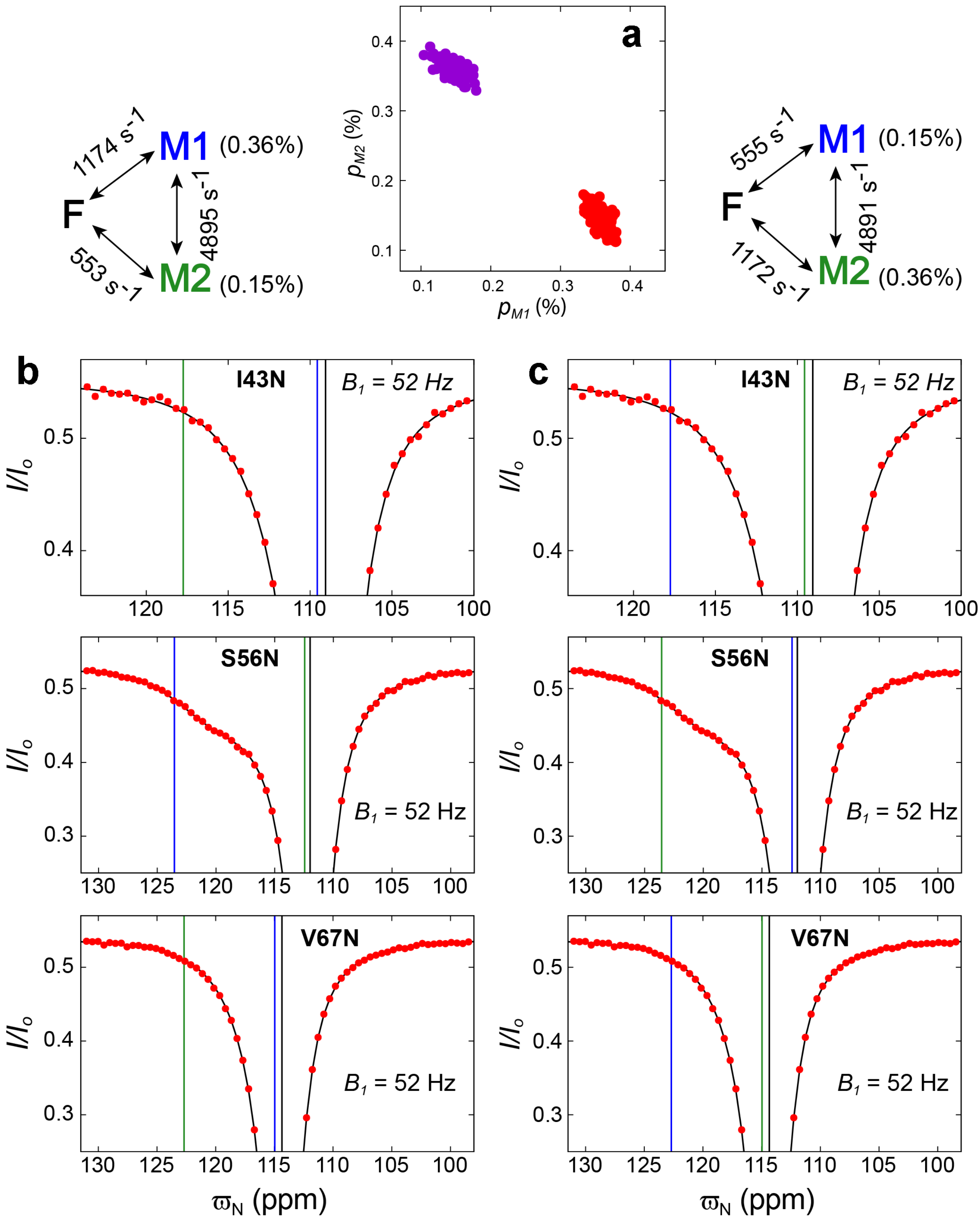

Fig. S1 Analysis of WT FF ^{15}N CEST data (15 °C) with i) $\Delta\varpi_{M1M2}$ constrained to be positive for K26, I43, V67 and Q68 and negative for S56 (red in a; b) and ii) $\Delta\varpi_{M1M2}$ constrained to be negative for K26, I43, V67 and Q68 and positive for S56 (purple in a; c). a) Distribution of best fit p_{M1} and p_{M2} values from 100 boot strap trials clearly shows that inverting the sign of $\Delta\varpi_{M1M2}$ interchanges the labels M1 and M2, but has no effect on the parameters of the exchange model. b,c) Best-fit three-state exchange model (black solid curves) to ^{15}N CEST profiles (red circles) when the sign of $\Delta\varpi_{M1M2}$ is constrained as defined in i (b) and in ii (c). The best fit ϖ_F, ϖ_{M1} and ϖ_{M2} values are indicated using black, blue and green lines, respectively. The positions of the lines also confirm that M1 and M2 have been interchanged between b and c.

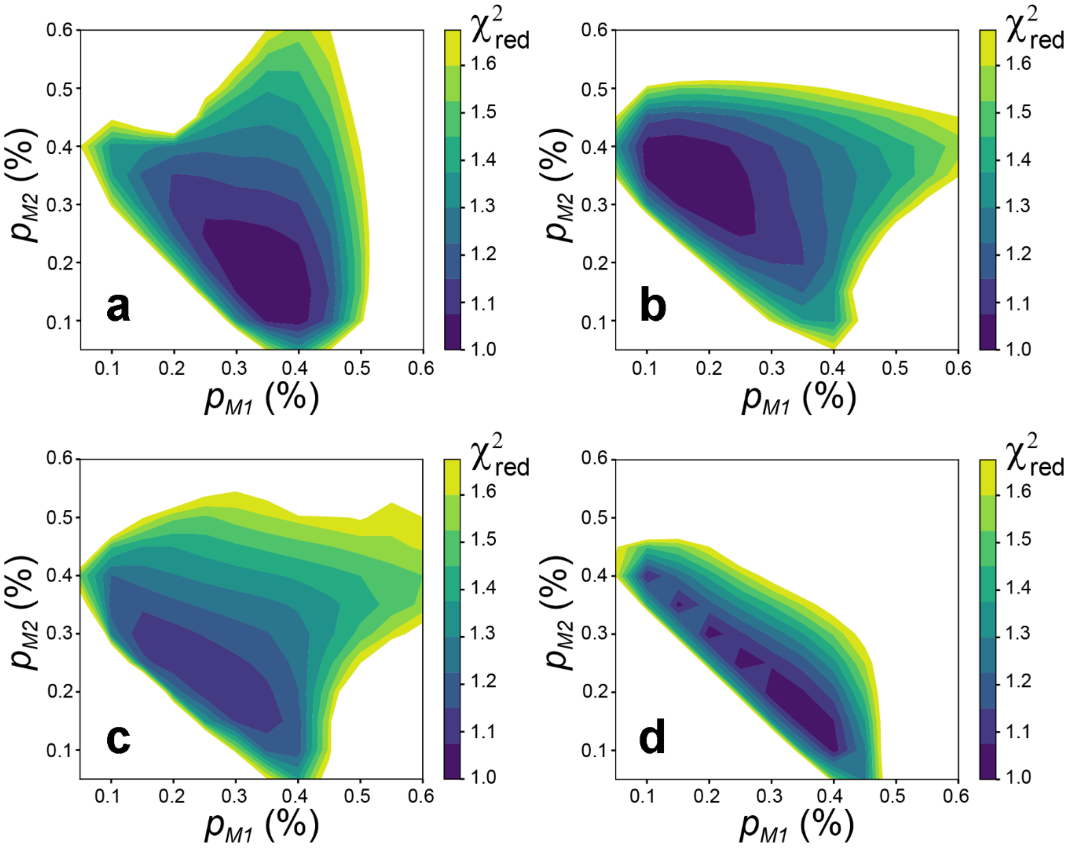

Fig. S2 χ^2_{red} as a function of p_{M1} and p_{M2} obtained from fits of CEST data subject to the constraint that (a) $\Delta\varpi_{M1M2} \geq 0$ for K26, I43, V67, Q68 and $\Delta\varpi_{M1M2} \leq 0$ for S56 or (b) $\Delta\varpi_{M1M2} \leq 0$ for K26, I43, V67, Q68, and $\Delta\varpi_{M1M2} \geq 0$ for S56, or (c,d) without any $\Delta\varpi_{M1M2}$ sign information. Plots in panels a, b, and c were calculated from fits of WT FF ^{15}N CEST profiles recorded at 15 ^{o}C using residues K25, I43, S56, V67 and Q68, while the plot shown in d was calculated using all set11 residues. It is clear that using the relative signs of $\Delta\varpi_{M1M2}$ in the analysis (a,b) leads to a single minimum in the χ^2_{red} surface and that inverting the sign of $\Delta\varpi_{M1M2}$ interchanges labels M1 and M2. In the absence of sign information for $\Delta\varpi_{M1M2}$ values (c), convergence to the correct p_{M1} and p_{M2} combination (as defined in a or b) does not occur as there are points in (c) that have higher values than in (a) and (b). Further, there are also spurious minima in (c) in which the χ^2_{red} values are less than in (a) and (b) because some of the $\Delta\varpi_{M1M2}$ values adopt the wrong sign. χ^2_{red} values plotted in (a), (b) and (c) were normalised by the minimum χ^2_{red} obtained when the five residues with sign information were analysed, and in (d) by the minimum when all 11 residues were included in fits (as is the case in the final panel). The multiple minimum problem (in the absence of the signs for $\Delta\varpi_{M1M2}$) is made clear in d.

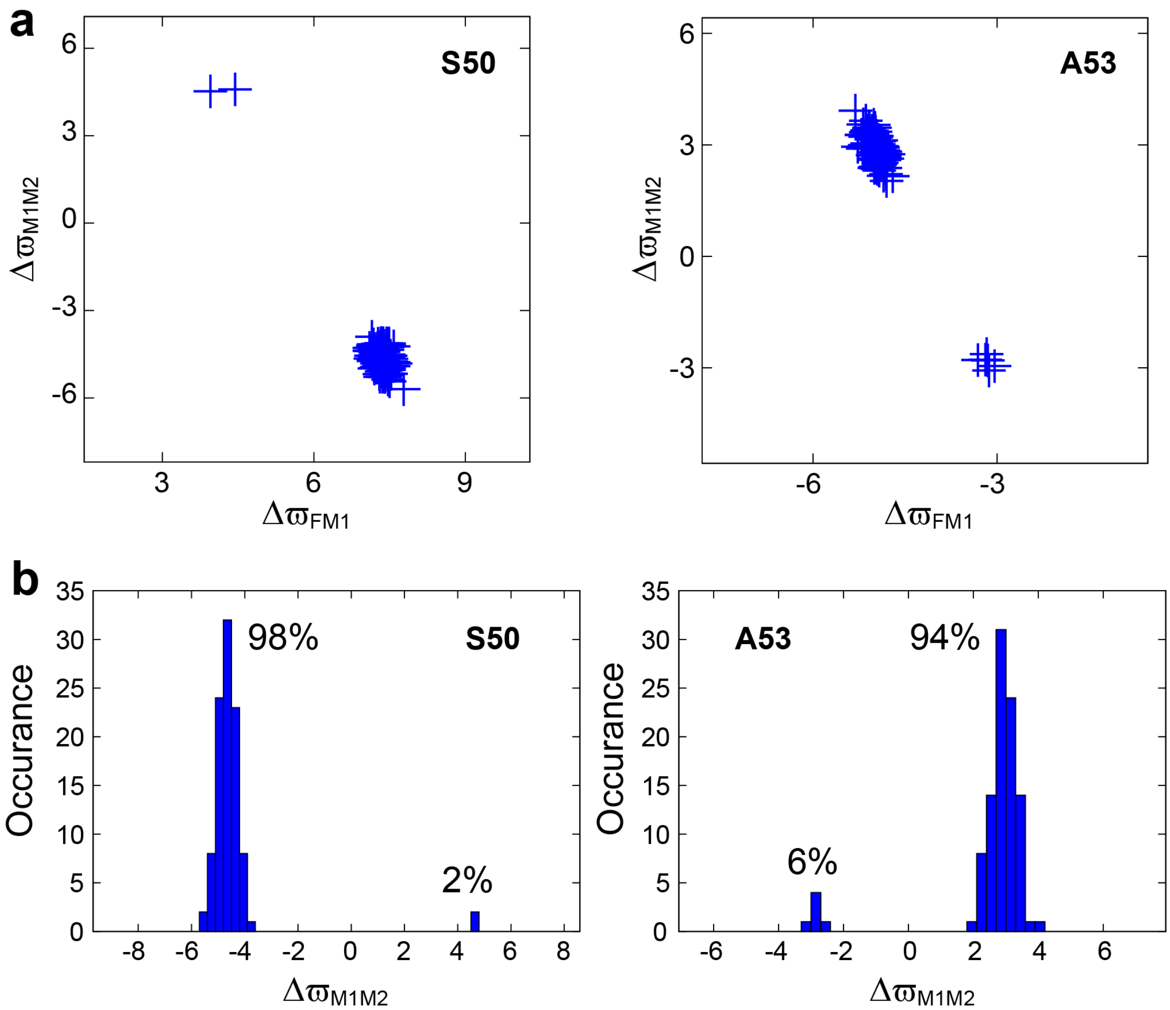

Fig. S3 Analysis of WT FF ^{15}N CEST data recorded at 20 °C for S50 and A53 to obtain the signs of the $\Delta\varpi_{M1M2}$ values for these residues. a) $\Delta\varpi_{M1M2}$ vs $\Delta\varpi_{FM1}$ plots from 100 bootstrap trials. b) Distribution of $\Delta\varpi_{M1M2}$ values from 100 bootstrap trials. The distribution of $\Delta\varpi_{M1M2}$ based on fits of data recorded at 20 °C is consistent with the corresponding distribution obtained by analysis of CEST profiles recorded at 15 °C (Fig. 8). The analysis was performed as described in the text for the 15 °C data. The best fit exchange parameters obtained from fits of the 20 °C ^{15}N CEST data using residues K26, I43, S56, V67 and Q68 are: p_{M1} = 0.55 ± 0.03 %, p_{M2} 0.2 ± 0.03 %, $k_{ex,FM1}$ = 1760 ± 81 s^{-1}, $k_{ex,FM2}$ = 425 ± 253 s^{-1}, and $k_{ex,M1M2}$ = 8430 ± 721 s^{-1}.

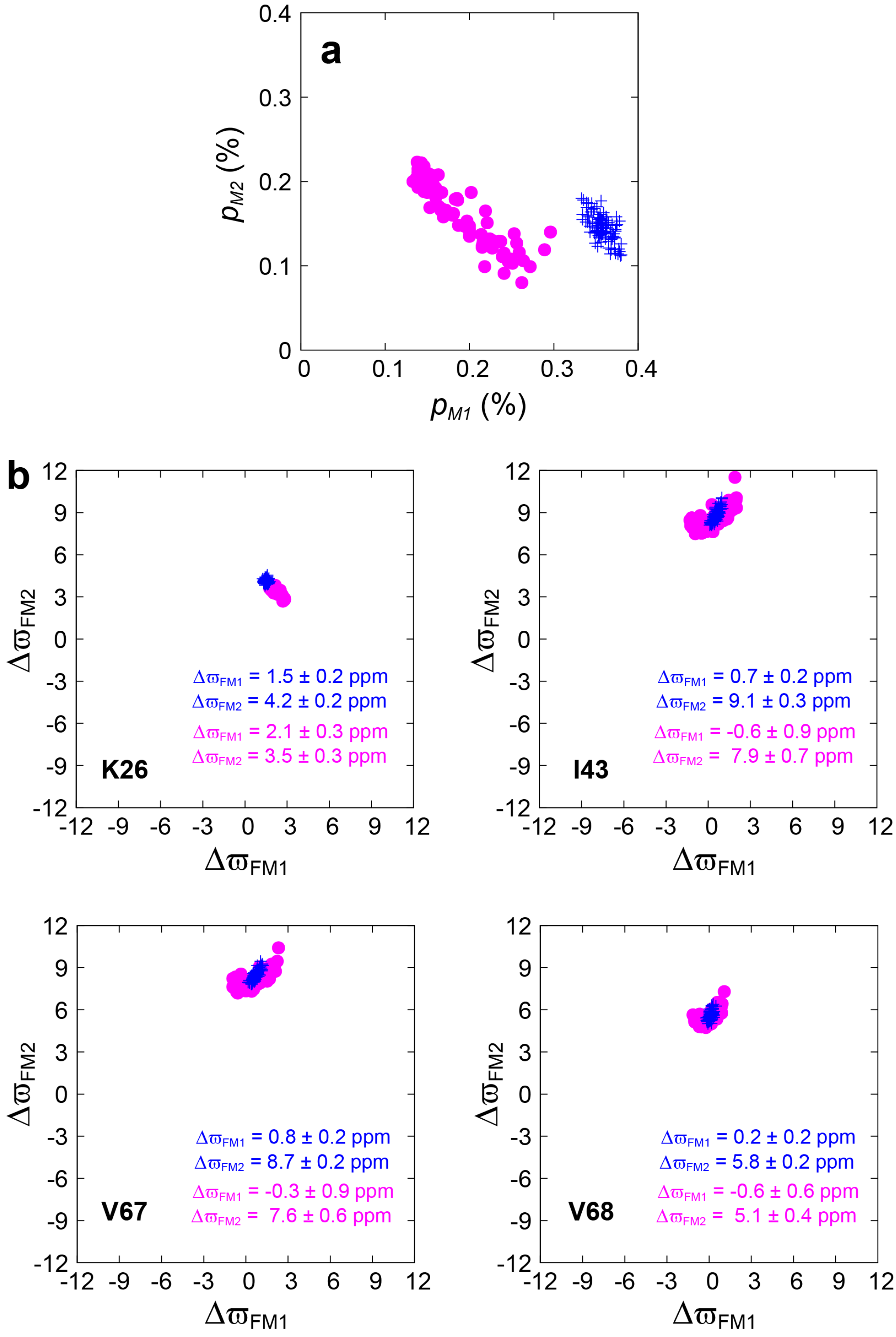

Fig. S4 a) p_{M1} and p_{M2} are not well defined when S56 is not included in the analysis of ^{15}N CEST data. p_{M1} and p_{M2} obtained from 100 bootstrap trials are shown when S56 was (blue) and was not (magenta) included in the data analysis. b) $\Delta\varpi_{FM1}$ and $\Delta\varpi_{FM2}$ obtained from 100 bootstrap trials are shown when profiles measured for S56 were (blue) and were not (magenta) included in the analysis. Data shown in blue is from Fig. 7 for comparison. The best fit (χ^2_{red} = 0.8) exchange parameters in the absence of data from residue S56 are $k_{ex,FM1}$ = 6 ± 374 s^{-1}, $k_{ex,FM2}$ = 1900 ± 290 s^{-1}, $k_{ex,M1M2}$ = 4992 ± 856 s^{-1}, p_{M1} = 0.14 ± 0.04 % and p_{M2} = 0.21 ± 0.04%. Note that these exchange parameters are significantly different than when S56 is included indicating that S56 is a critical residue in the analysis, but that reasonably accurate chemical shifts are, nevertheless, still obtained.

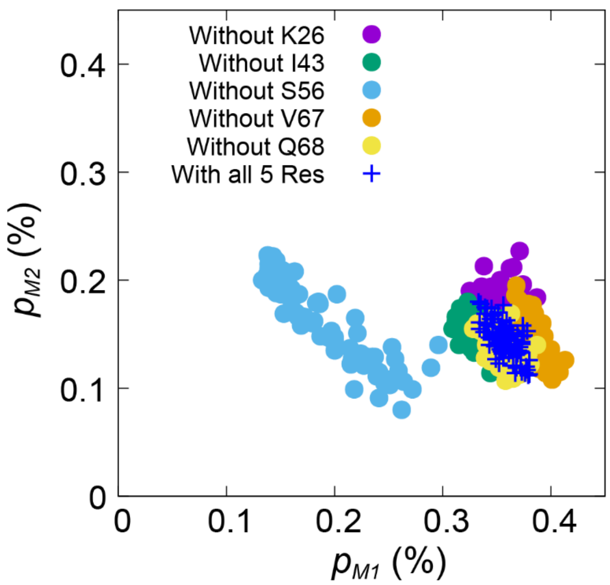

Fig. S5 Scatter plot showing the distribution of three-state p_{M1} and p_{M2} values obtained for WT FF (15 °C) when ^{15}N CEST profiles from four out of the five residues from set5 (the set of residues for which the sign of $\Delta\varpi_{M1M2}$ was available from temperature dependent CEST data) were analyzed. For reference the exchange populations obtained from an analysis of the ^{15}N CEST profiles from all five set5 residues (from Fig. 7) is also shown in dark blue (+). The p_{M1} and p_{M2} distributions were obtained from 100 bootstrap trials.

Expt No	Sample	Temperature (°C)	B_1 (Hz)	T_{EX} (ms)	ϖ_{CENT} (ppm)	Range (Hz)	Step (Hz)
1	WT FF	15	20.8	475	117.690	±1100	25
2		15	52.0	450	117.690	±1400	35
3		15	104.0	350	117.690	±1746	48.5
4		15	208.0	350	117.690	±1746	48.5
5		20	21.0	475	117.638	±1100	25
6		20	52.6	450	117.638	±1400	35
7		20	105.2	350	117.638	±1746	48.5
8		20	210.4	350	117.638	±1746	48.5
9		25	21.0	475	117.589	±1100	25
10		25	52.4	450	117.589	±1400	35
11		30	21.0	475	117.540	±1100	25
12		30	52.3	450	117.540	±1400	35
13		30	104.6	350	117.540	±1746	48.5
14		30	209.2	350	117.540	±1746	48.5
15	A39 FF	1	20.7	475	119.816	±1250	25
16		1	51.8	400	119.816	±1400	56
17		2.5	20.6	475	119.805	±1250	25
18		2.5	51.6	400	119.805	±1400	56
19		5	20.7	475	119.776	±1250	25
20		5	51.8	400	119.776	±1400	56
19		10	20.8	475	119.742	±1250	25
21		10	51.0	400	119.742	±1400	56
22		15	20.9	475	119.688	±1250	25
23		15	52.3	400	119.688	±1400	56

Table S1 Details of the ^{15}N CEST experiments recorded on the WT FF and A39G FF samples at 700 MHz (16.4 T). During T_{EX} the B_1 carrier was placed at a frequency within ±range (Hz) of ϖ_{CENT} for each 2D plane, with a carrier spacing between adjacent irradiation offsets of Step (Hz). To normalise the intensities an additional reference plane was recorded with T_{EX} set to 0 s.

Residue	ϖ_F (ppm)	$\Delta\varpi_{FI1}$ (ppm)		$\Delta\varpi_{FI2}$ (ppm)	
		Value	Error	Value	Error
K26	115.79	4.21	0.2	1.54	0.2
K41	114.01	4.25	0.2	2.33	0.2
I43	109.06	9.05	0.3	0.68	0.2
S50	108.00	3.71	0.2	6.94	0.2
L52	111.37	7.91	0.6	7.05	0.3
A53	126.28	-3.30	0.2	-4.48	0.2
S56	111.98	0.18	0.5	11.55	0.2
K59	116.31	6.28	0.2	3.37	0.2
V67	114.36	8.67	0.2	0.80	0.2
Q68	120.62	5.78	0.2	0.19	0.2

Table S2 WT FF folded state chemical shifts for residues from set10 (ϖ_F) along with the best fit $\Delta\varpi_{FI1}$ and $\Delta\varpi_{FI2}$ values obtained from the three-state analysis of ^{15}N CEST data (15°C). Minimum errors in the $\Delta\varpi_{FI1}$ and $\Delta\varpi_{FI2}$ values were set to 0.2 ppm.

Calculation No	Residues dropped	$k_{ex,FM1}$ (s^{-1})	$k_{ex,FM2}$ (s^{-1})	$k_{ex,M1M2}$ (s^{-1})	p_{M1} (%)	p_{M2} (%)
1	K26	1061 ± 80	768 ± 143	4676 ± 240	0.35 ± 0.01	0.18 ± 0.02
2	I43	1249 ± 60	468 ± 115	4353 ± 225	0.33 ± 0.01	0.15 ± 0.01
3	S56	6.0 ± 374	1900 ± 289	4992 ± 856	0.14 ± 0.04	0.21 ± 0.04
4	V67	1085 ± 74	800 ± 193	6168 ± 492	0.38 ± 0.01	0.15 ± 0.02
5	Q68	1245 ± 52	408 ± 132	4678 ± 208	0.35 ± 0.01	0.14 ± 0.01
6	None	1174 ± 63	533 ± 158	4895 ± 295	0.36 ± 0.01	0.15 ± 0.01

Table S3 Three-state exchange parameters obtained for WT FF at 15 ^{o}C when ^{15}N CEST profiles from four out of five set5 residues were analysed (calculations 1-5) using $\Delta\varpi_{M1M2}$ sign information. For reference the exchange parameters obtained from an analysis of the ^{15}N CEST profiles from all five set5 residues is also shown (calculation 6).